Annales Geophysicae

Evolution of dipolarization in the near-Earth current sheet induced by Earthward rapid flux transport

R. Nakamura[1], **A. Retinò**[1], **W. Baumjohann**[1], **M. Volwerk**[1], **N. Erkaev**[2], **B. Klecker**[3], **E. A. Lucek**[4], **I. Dandouras**[5], **M. André**[6], **and Y. Khotyaintsev**[6]

[1]Space Research Institute, Austrian Academy of Sciences, 8042 Graz, Austria
[2]Institute of Computation Modelling, Russian Academy of Sciences, Siberian Branch, Krasnoyarsk, Russia
[3]Max-Planck-Institut für extraterrestrische Physik, P.O. Box 1312, Garching, 85741, Germany
[4]Imperial College, London, SW7 2BZ, UK
[5]CESR/CNRS, 9 Ave. du Colonel Roche, B.P. 4346, 31028 Toulouse Cedex 4, France
[6]Swedish Institute of Space Physics, P.O. Box 537, 75121 Uppsala, Sweden

Abstract. We report on the evolution of dipolarization and associated disturbances of the near-Earth current sheet during a substorm on 27 October 2007, based upon Cluster multi-point, multi-scale observations of the night-side plasma sheet at $X \sim -10\, R_E$. Three dipolarization events were observed accompanied by activations on ground magnetograms at 09:07, 09:14, and 09:22 UT. We found that all these events consist of two types of dipolarization signatures: (1) Earthward moving dipolarization pulse, which is accompanied by enhanced rapid Earthward flux transport and is followed by current sheet disturbances with decrease in B_Z and enhanced local current density, and subsequent (2) increase in B_Z toward a stable level, which is more prominent at Earthward side and evolving tailward. During the 09:07 event, when Cluster was located in a thin current sheet, the dipolarization and fast Earthward flows were also accompanied by further thinning of the current sheet down to a half-thickness of about 1000 km and oscillation in a kink-like mode with a period of $\sim$15 s and propagating duskward. Probable cause of this "flapping current sheet" is shown to be the Earthward high-speed flow. The oscillation ceased as the flow decreased and the field configuration became more dipolar. The later rapid flux transport events at 09:14 and 09:22 UT took place when the field configuration was initially more dipolar and were also associated with B_Z disturbance and local current density enhancement, but to a lesser degree. Hence, current sheet disturbances induced by initial dipolarization pulses could differ, depending on the configuration of the current sheet.

Keywords. Magnetospheric physics (Plasma convection; Plasma sheet; Storms and substorms)
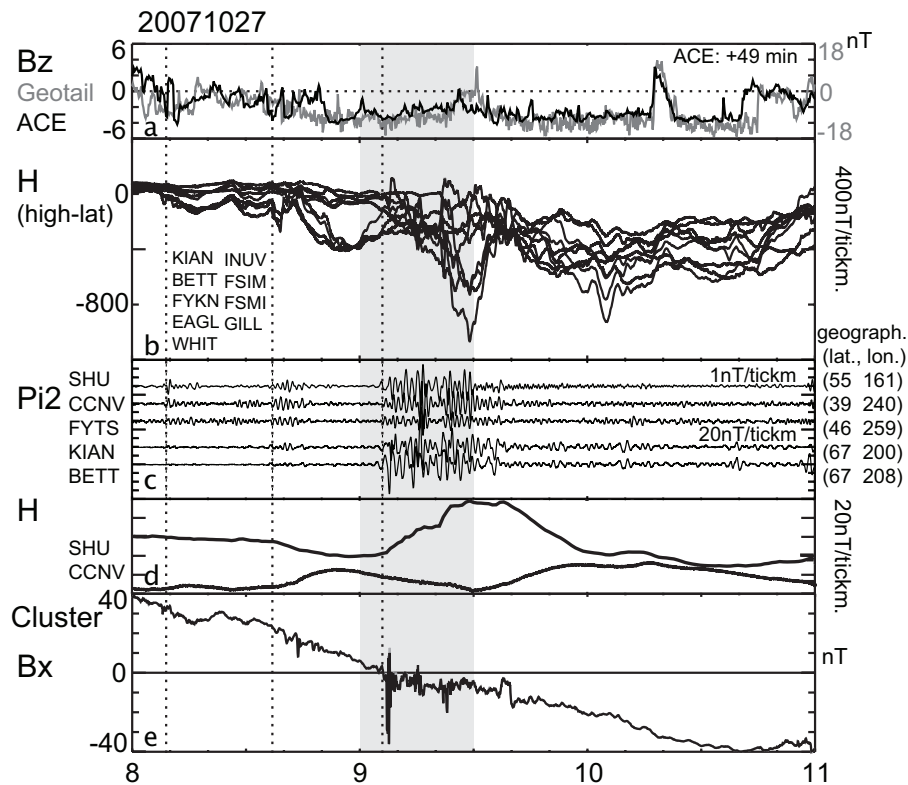
1 Introduction

One of the essential signatures of substorm onset observed in the magnetosphere is the magnetic field dipolarization, i.e., enhancement(s) in B_Z, indicating that the distribution of the tail current has changed locally and/or globally. Statistical studies of dipolarization events using satellites between 6.4 and 17 R_E downtail showed that more events were observed further away from Earth (Lopez et al., 1988; Sigsbee et al., 2005). Many studies reported that dipolarization are associated with Earthward flows exceeding 100 km/s and attributed to magnetic flux transported Earthward (e.g., Angelopoulos et al., 1994; Baumjohann et al., 1999; Sigsbee et al., 2005). The dipolarization happens first in a limited region and propagates azimuthally (e.g., Nagai, 1982) as expected also from the finite width of the fast flows and accompanying magnetic disturbances (e.g., Sergeev et al., 1996; Nakamura et al., 2002, 2004). On a long time scale ($\sim$45 min), however, the dipolarization propagates tailward recovering globally from a thin current sheet state to a dipolar configuration (Baumjohann et al., 1999).

One mechanism for dipolarization is that the near-Earth neutral line (NENL) causes large amounts of magnetic flux to be transported Earthward, which eventually starts to pile

Correspondence to: R. Nakamura
(rumi.nakamura@oeaw.ac.at)

Fig. 1. (a) IMF B_Z from ACE and B_Z component from Geotail in the magnetosheath at $(X, Y, Z)=(-2, 16, 13)\,R_E$, **(b)** H component of the high-latitude magnetograms from north-American stations, **(c)** mid-latitude and high-latitude Pi2 (filtered H component between 40 and 150 s), **(d)** positive bay, and **(e)** B_X component of C3. The three positive bay onsets discussed in the text are shown by the vertical line. The gray hatched time shows the third substorm event when Cluster crossed the center of the current sheet.
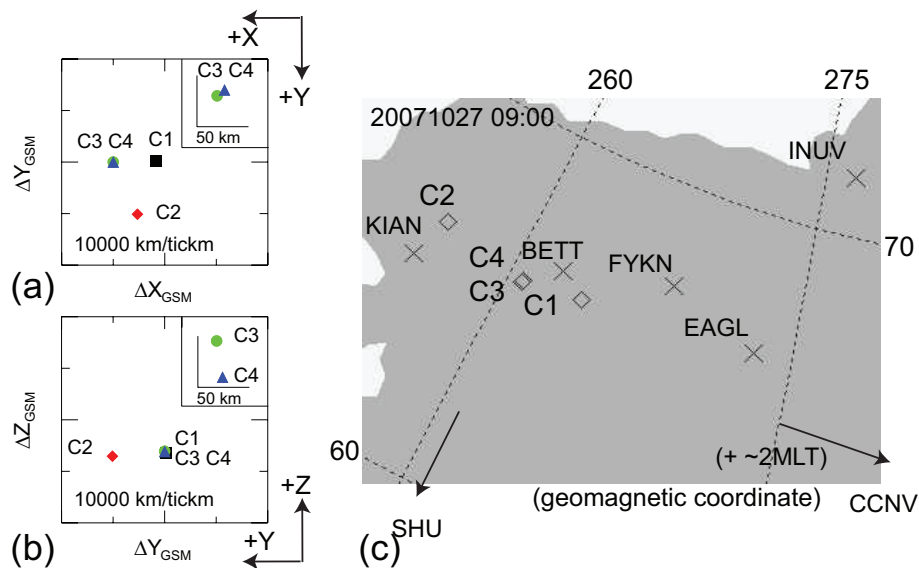
up in the near magnetotail region where the flows brake in a strong field/high pressure region (Shiokawa et al., 1997; Baumjohann, 2002). Such pile-up effect is expected to propagate tailward (e.g., Birn and Hesse, 1996). Tailward and azimuthal propagation of the magnetic disturbance is also a natural direction, when instabilites such as ballooning (Roux et al., 1991) or cross-field current instabilities (Lui et al., 1991) take place near Earth dipolar region. To study the evolution of the near-Earth current sheet disturbances during a substorm dipolarization and to examine the role of the flux transport from the tail, propagation properties of the field and those of the flow disturbances need to be examined independently.

Since July 2007 Cluster started to observe the magnetotail neutral sheet regions Earthward of $11\,R_E$, where fast flow braking is considered to take place (Shiokawa et al., 1997). A result from the four spacecraft analysis of the current sheet disturbance induced by the rapid flux transport observed from 09:07 UT on 27 October 2007 is studied in this paper. By analyzing the plasma and magnetic field data from Cluster we succeeded to measure the motion of the dipolarization front associated with the flow distur-

bances. While a pair of spacecraft was separated by only several 10s of km, the other two spacecraft and the pair were separated by 10 000 km from each other. This configuration allows to monitor the evolution of the fast flows associated disturbances at multi-scales. In this study we use Cluster data from the FluxGate Magnetometer (FGM) experiment (Balogh et al., 2001), the Electric Field and Wave (EFW) instrument (Gustafsson et al., 2001), and by the Cluster ion spectrometry (CIS) experiment (Rème et al., 2001).

2 Overview of the event

Between 08:00 and 11:00 UT on 27 October 2007, there are mainly three Pi2 activities accompanied by electrojet activations starting at around 08:08, 08:38, and 09:06 UT, as shown in Fig. 1. The 09:06 UT activation has the strongest electrojet and Pi2 when Cluster crossed the center of the current sheet (Fig. 1e) and will be discussed in this study. Cluster was located premidnight at $X_{\mathrm{GSM}}=-9.2\,R_E$, $Y_{\mathrm{GSM}}=5.5\,R_E$, $Z_{\mathrm{GSM}}=-1.6\,R_E$ with their foot points in the Alaskan sector. The relative position of the four spacecraft and location of the foot points are given in Fig. 2. The midlatitude
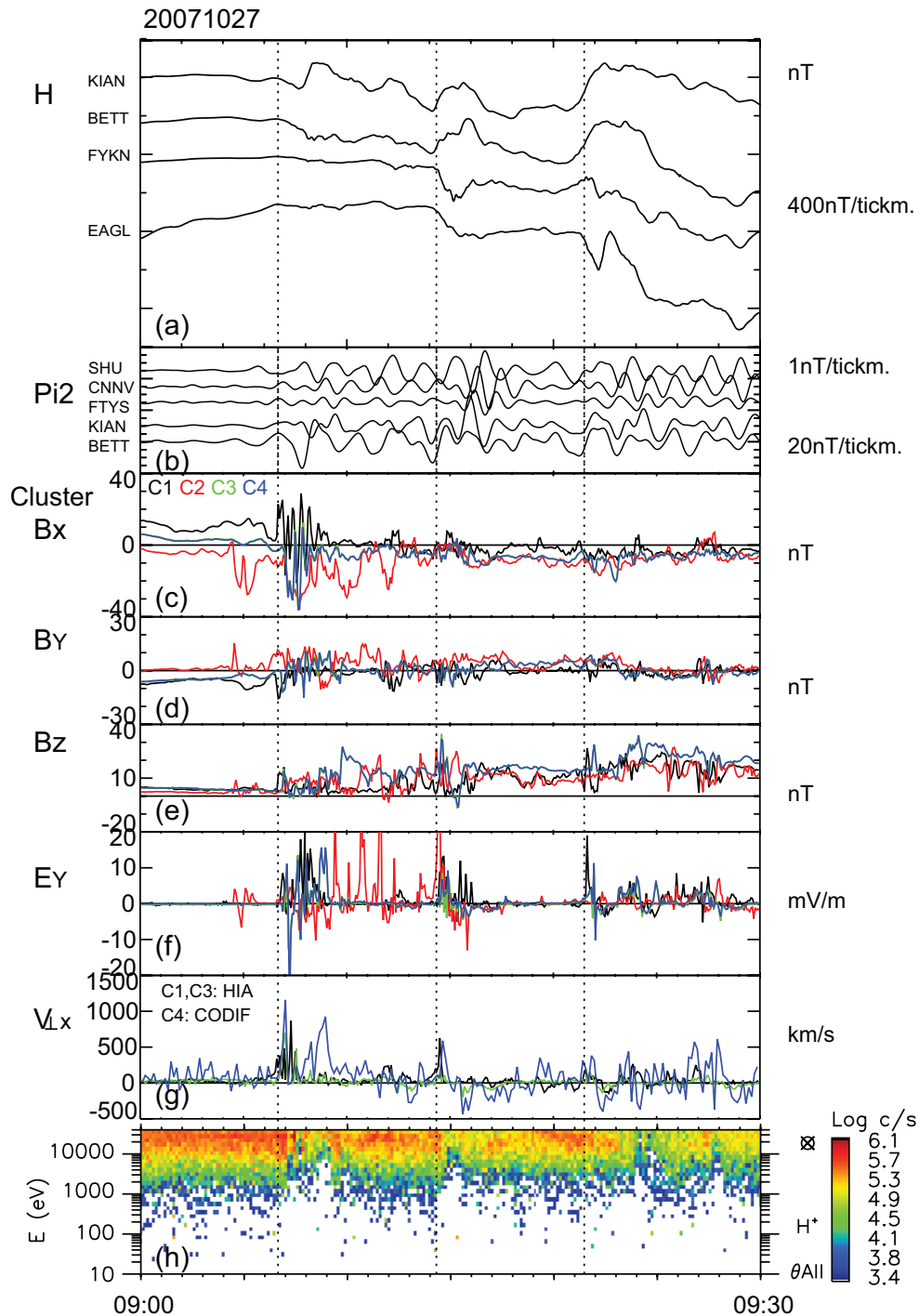
Fig. 2. Relative position of Cluster in **(a)** X-Y, **(b)** Y-Z plane, and **(c)** location of the foot-points of Cluster.

positive bay at SHU, located near the local time sector of Cluster, started around 09:06 UT with further enhancement at 09:25 UT, while the positive bay at CCNV, located about 1.5 MLT east of WHI, started around 08:40 and 09:30 UT. This suggests that while the 08:38 UT onset is localized in Central American sector, the 09:06 UT onset is localized initially in Alaskan sector, but extends later to a larger local time sector involving Central American sector. This substorm occurred during a prolonged interval of negative IMF B_Z based on ACE and Geotail data (Fig. 1a).

Figure 3 shows the ground magnetogram and Cluster observations between 09:00 and 09:30 UT. Multiple intensifications in electrojet accompanied by Pi2 were detected at around 09:07, 09:14 and 09:21 UT as shown in Fig. 3a and b. All these intensifications are associated with dipolarizations, sudden enhancements in B_Z, and enhancements in E_Y exceeding 10 mV/m at Cluster (Fig. 3d and e). For plasma and field values Geocentric Solar Magnetospheric (GSM) coordinates are used unless stated otherwise. In this paper we use only the E_Y component in the Despun System Inverted (DSI) coordinate system. EFW measurement obtains the two components, E_X and E_Y, in this coordinate system, which is approximately Geocentric Solar Ecliptic (GSE) coordinate. Here we refer to E_Y as a proxy of the electric field component responsible for rapid flux transport or motion of the current sheet. The vertical lines indicate the starting times of the B_Z enhancement at Cluster 1, which are at 09:06:40, 09:14:20 and 09:21:30 UT. The strongest westward electrojet was observed at BETT, which was located near the foot points of C1,3,4 for the 09:07 UT event, while the foot point of C2 was located further west at the meridian of KIAN (Fig. 2c). Auroral observations around

the 09:07 event are discussed by Asano et al. (2009) using Polar UV images. A localized short-lived auroral activation started dusk side of the foot point of C2 between 09:04:18 and 09:04:55 UT and weakened while a next stronger activation started between 09:06:45 and 09:07:22 UT around the Cluster foot point regions. The strongest westward electrojet for the 09:14 UT and 09:21 UT activations were observed at FYKN and EAGL, respectively, indicating that the center of the electrojet region moved eastward of the Cluster foot point region. (Note that the foot points of Cluster during the 09:21 UT events are located about 5° west from those given in Fig. 2c.) Yet, BETT as well as KIAN still observed Pi2 as well as electrojet during the major electrojet activity from 09:21 UT, while negative bay at FYKN reached up to 1000 nT. The electrojets were stronger and involved a wider local time region compared to the 09:07 UT activation so that Cluster foot points were still within the active region of the electrojet during these later onsets.
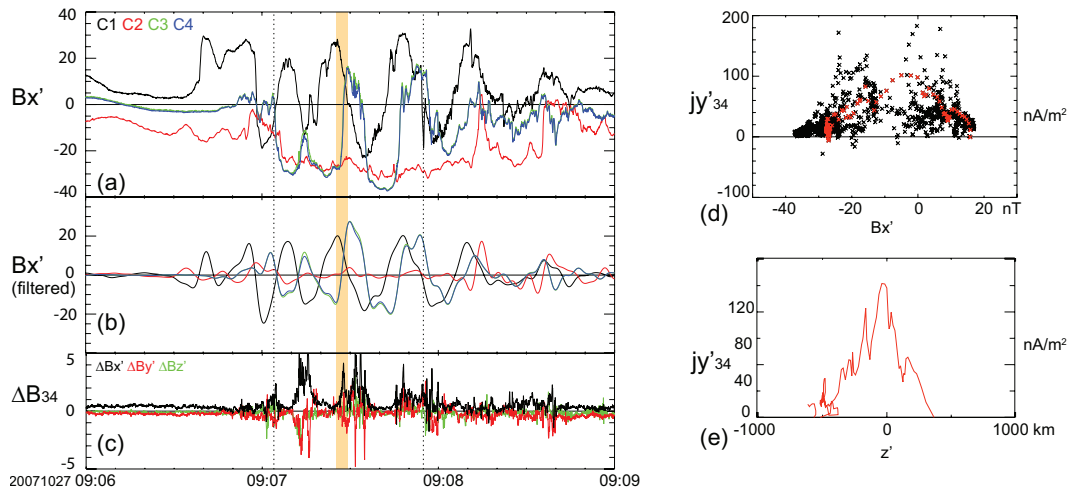
Cluster measurements during the substorm is summarized in Fig. 3c–h by showing 4s averaged data. While all the onsets were associated with dipolarization at Cluster in the plasma sheet with enhanced flux transport rate (E_Y), the current sheet configuration and therefore the disturbance characteristics are quite different among the three events. Before the 09:07 UT onset, C1 was in the Northern Hemisphere plasma sheet, while C2 was in the Southern Hemisphere plasma sheet, the pair C3-C4 was close to the center of the current sheet. Gradual decrease in B_Z, indicating stretching of the current sheet, was observed before the 09:07 onset (Petrukovich et al., 2009), which was identified as a typical feature of growth phase before a local activation onset of the current sheet. C2 started to observe recurrent negative

Fig. 3. (a) H-component from selected high-latitude stations, **(b)** Pi2, **(c–e)** three components of the magnetic field and **(f)** E_Y from the four Cluster, and **(g)** X component of the perpendicular plasma flow relative to the magnetic field from C1,C3, and C4, and **(h)** energy spectra for proton from C4. The three vertical line denotes the onset time of dipolarization at C1, i.e., 09:06:40, 09:14:20, 09:21:30 UT.

excursion of B_X from 09:04 UT with 2–3 min scale lasting until the next onset at 09:14 UT. The disturbance therefore started preceding a clear onset in the electrojet as shown in Fig. 3, but could be related to the localized auroral activation that appeared between 09:04:18 and 09:04:55 UT west of C2 foot point. The enhancement in B_Z during the 09:07 onset
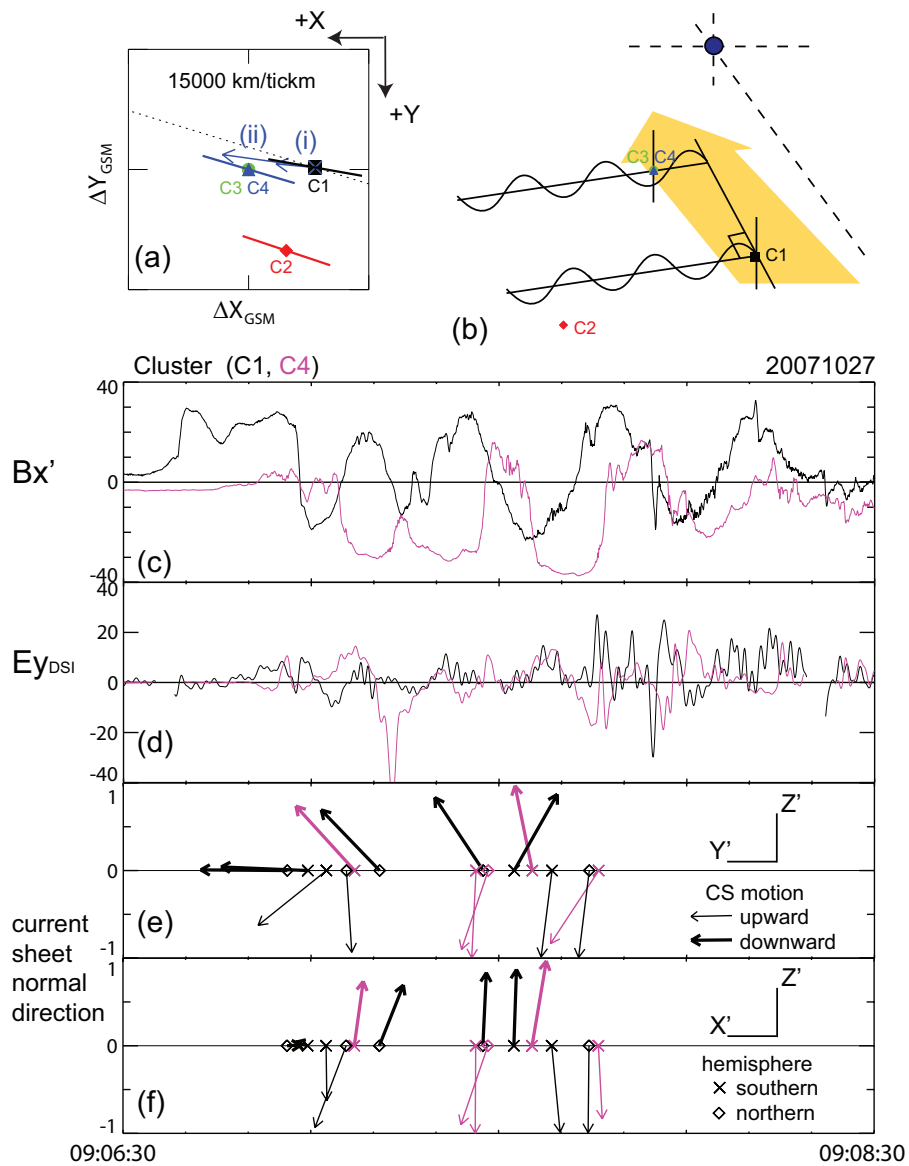
Fig. 4. (a) 22-Hz data of B_X', (b) band-pass filtered data between 5 s–30 s period, and (c) the difference of the three components of the magnetic field between C3 and C4. Modified coordinate system discussed in the text is used. (d) j_Y' profiled relative to B_X' between 09:07:04 and 09:07:55 UT estimated from C3 and C4 data by assuming that the difference in B_X' represents the gradient in Z' direction. (e) Spatial profile of the current density along Z' estimated during the current sheet crossing between 09:07:24 and 09:07:29 UT.

is accompanied by enhanced electric field disturbances, and enhanced fast flows, and current sheet oscillations with about 15 s period in C1,C3 and C4. As shown in the CODIF energy spectra plot (Fig. 3h), the energy range of the plasma sheet components exceed the instrument energy range. The velocity dip between 09:07–09:08 UT is therefore most likely instrumental effect. Nonetheless, combined with the enhanced E_Y it can be seen that these current sheet disturbances are associated with Earthward fast flows. No oscillations were observed during the dipolarization for the 09:14 and 09:21 UT onsets, where the initial values of B_Z were larger. The fields and flow data again showed that these onsets are also associated with enhanced Earthward flows and E_Y. An important characteristic is also that all these three dipolarization events start with the signature from C1, which was located most tailward among the four spacecraft (Fig. 2a). The overall B_Z and B_X profiles, including the smaller interspacecraft differences for later onsets, suggest that the current sheet was thinner and more stretched during the 09:07 UT event at Cluster compared to the thicker plasma sheet for the 09:14 and 09:22 UT onsets. We examine the detailed characteristic of the current sheet for the 09:07 UT onset, when Cluster was located most conjugate to the central meridian of the ground activity, in Sect. 3 and discuss the current sheet dynamics during the three dipolarization events based on multi-point observations in Sect. 4. Characteristics of the acceleration and transport processes of electrons during the entire substorm are described by Asano et al. (2009).

3 Current sheet disturbance associated with fast flows (09:07 event)

Figure 4 shows the expanded view of the current sheet oscillation. Here we use a new coordinate system, where X' and Y' axis are tilted by 17° clockwise in the X_{GSM}-Y_{GSM} plane viewed from the north. In this new coordinate system the X' direction is the maximum variance (MaxVar) direction of the magnetic field for C3 and C4 between 09:06–09:09 UT, which was almost parallel to the X_{GSM}-Y_{GSM} plane. The X' direction represent the MaxVar direction also for the other spacecraft, as can be seen in Fig. 5a, where the MaxVar direction of the four spacecraft are plotted together with the X' direction. The deviation here is less than 7°. Although some high-frequency disturbance is overlapped, Fig. 4a shows clear oscillation in $B_{X'}$ component with frequency of about 15 s for C1,C3 and C4. The 15-s component becomes visible also in C2 when the data is filtered between period of 5 s and 30 s (Fig. 4b). The phase difference between C1 and C4/C3 changes slightly at later times. It is interesting to note that the duration of this wave activity is about the time scale of the negative excursion in $B_{X'}$ at C2. The amplitude of the 15 s-oscillation in $B_{X'}$ observed by C1 and C3,C4 has comparable value to the amplitude of the negative $B_{X'}$ excursion at C2. This indicate that the current sheet, at least where Cluster was located, became thin during the time interval when the 15-s oscillation was observed.

In addition to these general properties of the wave, the C3-C4 pair gives an estimate of the local current density. Without any assumption from the orientation of the current, the linear gradient in a 3-D space can only be determined using the four-spacecraft technique. Yet, with two spacecraft

Fig. 5. (a) CODIF proton flow vector at (i) 09:06:53 and (ii) 09:07:01 UT and the maximum variance direction for the four spacecraft. The dotted line shows the X' axis direction. **(b)** Schematic drawing showing the relationship between the fast flows and current sheet oscillation. **(c)** B'_X and **(d)** 1s averaged E_Y from C1 and C4 between 09:06:30 and 09:08:30 UT. Normal direction of the current sheet for each half-hemisphere crossings projected on the **(e)** Y'-Z' plane and the **(f)** X'-Z' plane.

and with a knowledge of the average orientation of the current sheet, which in our case is parallel to the X'-Y' plane, we can still examine the current sheet structure using differences between C3 and C4 as shown in Fig. 4c. Note that these two spacecraft are separated mainly in Z direction (Fig. 2a and b). Here $\Delta B_{X'}$ is expected to represent the tail current density and $\Delta B_{Y'}$ the field-aligned current. It can be seen that from 09:06:50 UT, starting with the enhancement in $B_{X'}$ disturbance, the differences become larger. Note that the largest difference is in $\Delta B_{X'}$ component, which is expected to show the enhancement in the tail current sheet density, while there are also some peaks in $\Delta B_{Y'}$. $\Delta B_{Z'}$ is generally a minor component except during the spiky enhancements around 09:07:02 and 09:07:12 UT. Dawn-to-dusk current density profile, $j_{Y'} = \Delta B_{X'}/\Delta Z'$, along the current sheet, $B_{X'}$, during the first three periods of oscillations, i.e. between 09:07:04 and 09:07:55 UT, is shown in Fig. 4d. It can be seen that the data points of large current density are distributed on both sides of the current sheet between $B_{X'}=-15$ nT and $B_{X'}=15$ nT. These periods of high current density are most

likely ascribed to some transient/localized disturbance of the current filaments. As expected the peaks in $\Delta B_{Y'}$ and $\Delta B_{Z'}$ took place also during some of these large $\Delta B_{X'}$ intervals. There is, however, one rather simple current sheet crossing between 09:07:24 and 09:07:29 UT when a monotonic increase in $B_{X'}$ was observed without spiky signatures, suggesting a rapid enough crossing to assume a steady spatial structure during the crossing. By assuming that the observed temporal change is due to a spatial structure, we estimated the velocity of the crossing and hence the $j_{Y'}$ along Z' as shown in Fig. 4e. It can be seen that the scale size of this oscillating current sheet is about 1000 km. Note that this is about the separation of the Cluster tetrahedron in Z direction.
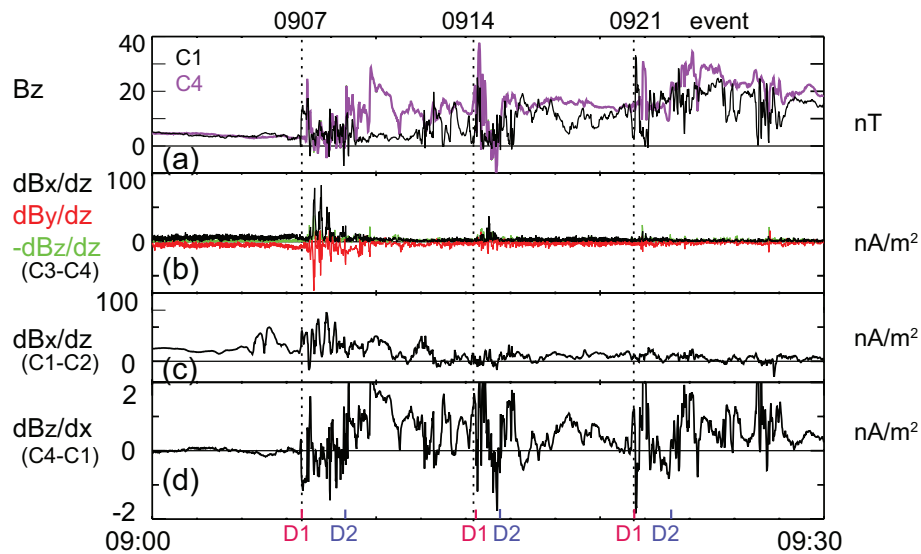
To examine the characteristics of the oscillations we compared the motion of the current sheet for the two spacecraft C1 and C4 in more detail as shown in Fig. 5c–f. (Here C3 and C4 give exactly the same results in terms of this large scale structure, while the oscillation at C2 is less clear and is therefore excluded from the analysis). First we compare the $B_{X'}$ and E_Y profiles. The general E_Y pattern gives the oscillatory signatures with reversal from positive to negative excursion in E_Y around the negative and positive peak of $B_{X'}$, at least for the first 3–4 periods. Such a pattern arises when there is an up-down motion of the current sheet with an inward convection pattern, as was also observed in the flapping current sheet by Sergeev et al. (2003). Yet, it should be noted that larger E_Y variations, such as those around 09:07:12 UT, are not due to this current sheet motion but could be more due to E_Y variations in the current sheet frame, possibly due to the transient/localized filamentary structures discussed before. Furthermore, a rapid flux transport is expected to contribute to the E_Y profile. Here the time-scale of the oscillation is too short to confirm the motion using plasma data. To examine the oscillation characteristics, we performed the minimum variance (MinVar) analysis of the magnetic field data for each crossing of one half-hemisphere for all the up and down motion of the current sheet whenever relatively simple monotonic profile in B_X were observed. Figure 5e and f shows the direction of the well resolved MinVar direction (when the intermediate-to-minimum eigenvalue ratio exceeds 3). Their projections to the Y'-Z' (X'-Z') plane are displayed in Fig. 5e (f). These directions are expected to correspond to the normal of the current sheet. Here the thick (thin) arrows are used for those crossings when B_X' is decreasing (increasing), i.e. downward (upward) motion of the current sheet relative to spacecraft (alternatively upward (downward) motion of the spacecraft relative to the current sheet) and are plotted in the upper (lower) half of Fig. 5e and f. The crosses (diamonds) show the data from the Southern (Northern) Hemisphere. Except for two half-hemisphere crossing events in C1 (corresponding to the second black thin arrow and the last thick arrow), all the arrows in Fig. 5e show the same direction of Y' at the upward/downward phases of the flapping oscillation with the same sense in the northern and southern halves of the current sheet during each phase.

No systematic behavior was obtained in the X'-Z' plane for these vectors (Fig. 5f), which had also smaller X' components. The same Y' direction for the upward and downward phase in the Y'-Z' plane implies a wavy current sheet and the same sense in the Northern Hemisphere and Southern Hemisphere region implies that the sheet is tilted as a whole. This suggests that the oscillations are a kink mode rather than a sausage mode wave, which was also for the current sheet case studied by Sergeev et al. (2003) but for a longer time-scale (3–4 min) oscillation.

Since this flapping is exclusively observed during the fast flow interval, it is important to compare the ion motion and the propagation of the wave to identify its characteristics. Figure 5a also shows the two sequences of plasma flow obtained by CODIF from C4 at (i) 09:06:53.4 and (ii) 09:07:01.7 UT. Note that the flows at time (i) and (ii) are obtained when C4 was at equator with enhanced B_Z and are therefore mainly perpendicular flows. As can be seen in Fig. 5a, the fast flow vectors, (i) and (ii), are both nearly aligned and are Earthward and dawnward in GSM coordinates and close to the X' direction, which is dawnward by about $10°$ from the flow direction. From the results of the minimum variance analysis (Fig. 5e–f) and the relative direction of the flows and MaxVar direction (Fig. 5a), we can conclude that the wave is propagating perpendicular to the field, along the current direction, i.e. Y', which is also nearly perpendicular to the fast flow as illustrated in Fig. 5b. Using the time difference in the flapping between C1 and C4, i.e., the first negative excursion in B_X during the flapping wave event, which is 7 s, we obtain the observed propagation velocity to be 380 km/s along Y' direction. With the 15 s period, this will result in a wavelength of 5700 km. The propagation velocity is somewhat higher than the observed ion velocity in the Y' direction, i.e., 180 km/s. Taking into account the Doppler shift due to this ion motion, the wave period is estimated to be 28 s.

4 Dipolarization and change in the current sheet configuration

All the three dipolarization events were associated with enhanced B_Z and Earthward fast flow, followed by some fluctuations in the current sheet. Figure 6 summarizes the current sheet characteristics during the three dipolarizations by comparing the magnetic field difference among different spacecraft. Figure 6b shows the gradient obtained from C3 and C4. As discussed before, C3 and C4 are separated predominantly in the Z direction, i.e., $(\Delta X, \Delta Y, \Delta Z)=(7, 5, 35)$ km. We can interpret $\Delta B_X/\Delta Z$ to represent j_Y, which corresponds to the local tail current density and $\Delta B_Y/\Delta Z$ representing $-j_X$, which is a reference value of the local field aligned current (FAC) density. It can be seen that for the first two dipolarizations there is clear enhancement detected in the local current density, while there is some enhancement but
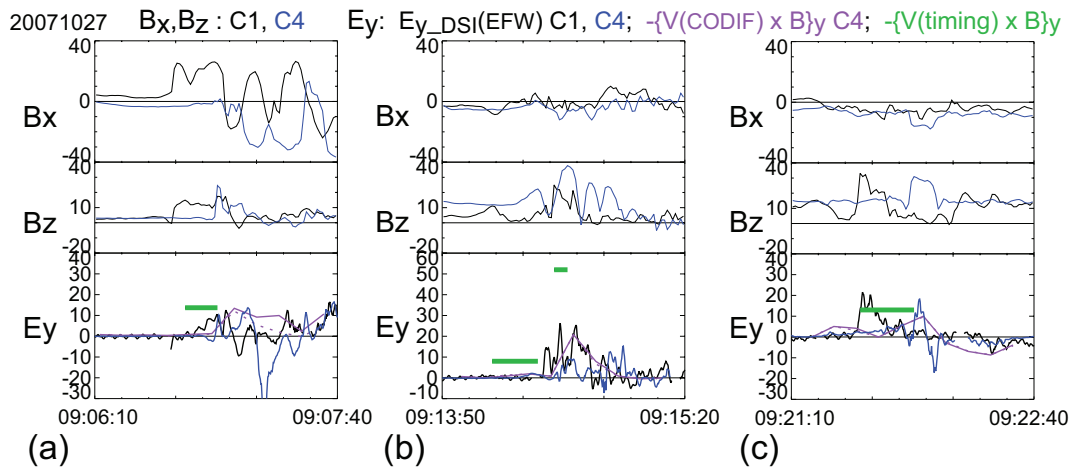
Fig. 6. Characteristics of the current sheet between 09:00 and 09:30 UT. (a) B_Z from C1 and C4, (b) magnetic field gradient obtained from C3 and C4 assuming that the main gradient direction is across the current sheet, i.e., Z, (c) $\Delta B_X / \Delta z$ using C1 and C2, and (d) $\Delta B_Z / \Delta x$ using C1 and C4.

rather minor one for the 09:21 UT event. The 09:07 UT event shows in addition to the enhancement in the tail current density, a comparable negative excursion in $\Delta B_Y / \Delta Z$, which corresponds to an Earthward current. This current density enhancement might suggest downward current of the current wedge. Yet this direction of j_X is an unexpected direction of the current wedge type FAC associated with a localized fast flow, since the flow as well as field disturbances were more prominent at the meridian of C1,C3,C4 compared to C2, suggesting that Cluster was more likely at the western side of the current wedge (in upward FAC region). Earthward FAC has been also frequently observed in the plasma sheet at the outer (off-equatorial) part of a fast flow and one possible interpretation is the continuation of the inflow current toward the reconnection region tailward of the spacecraft (Snekvik et al., 2008). The observed relatively thin current layer identifiable with C3 and C4 could support this interpretation. For the later dipolarization, however, there is less enhancement in the local current density suggesting that Cluster is engulfed in a thicker plasma sheet and most likely gradients along Z becomes less important.

While the local current signatures can be examined from the C3-C4 relationships, the current sheet structure on a somewhat larger scale can be examined by comparing spacecraft with larger scale separation. As shown in Fig. 3c, C1 and C2 were located at the opposite side of the current sheet before the first event and most of the time detected the largest difference in B_X. The B_X difference, shown in Fig. 6c can therefore provide an average tail current density. It can be seen that the current density level, initially detected before the event, decreased after the three dipolarization. This in-

dicates redistribution of the current either due to thickening or disruption. Another striking feature is the 2–3 min oscillation observed at the beginning of the event. As discussed before B_X profile of C2 (see Fig. 3c) between 09:04 UT and 09:13 UT shows repetitive 2–3 min time scale negative B_X excursions when the spacecraft stayed in the Southern Hemisphere. Positive (negative) B_X excursion in Northern (Southern) Hemisphere is also seen in other spacecraft overlapped with the 15-s oscillation discussed above. For example, C1 observed first positive B_X excursion in the Northern Hemisphere at similar time scale when C2 observed negative excursion before starting the 15 s oscillation. The recurrent enhancements of the current density with 2–3 min scale seen in Fig. 6c is therefore due to the negative excursion in the Southern Hemisphere and positive excursion in the Northern Hemisphere, suggesting sausage mode, which have been seldom observed by Cluster for this time scale of oscillation (Sergeev et al., 2003; Runov et al., 2005b).
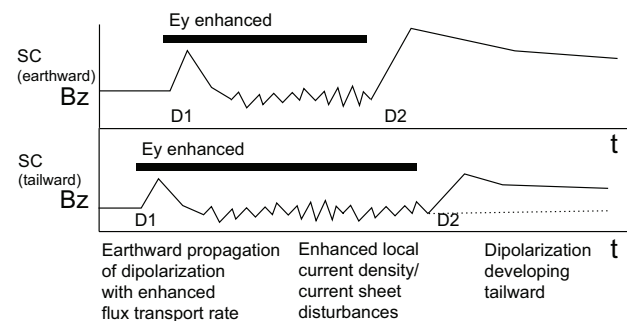
The gradient scale of B_Z is an essential parameters for the braking of the fast flow since the enhanced pressure in the dipolar region has been considered to be the cause of the flow braking (Shiokawa et al., 1997). Figure 6d shows the gradient of $\Delta B_Z / \Delta X$ using C1 and C4 data, since these spacecraft were separated mainly along the X direction. All the three events have similar patterns in the evolution, i.e. two phases in dipolarization. It can be clearly seen that the dipolarization is associated with negative excursion of the gradient, meaning that the initial signatures of the dipolarization starts always from C1, which is consistent that the flux is transported Earthward. This negative gradient is associated with the enhanced electric field/fast flow observation. Enhancement in

Fig. 7. B_X and B_Z from the four Cluster spacecraft and E_Y estimated from different methods during the three dipolarization events: **(a)** 09:06:10–09:07:40 UT, **(b)** 09:13:50–09:15:20 UT, and **(c)** 09:21:10–09:22:40 UT.

B_Z takes place in a rather transient manner and is followed by a decrease in B_Z for both spacecraft (first dipolarization, marked as D1 in Fig. 6d) with enhanced fluctuations and also enhance local current density (Fig. 6b). For the 09:07 UT event, current sheet oscillation was detected during this period of low B_Z. For 09:14 UT event and 09:21 UT event, however, more higher frequency disturbances were observed. A turning into more stable positive gradient due to enhancement in B_Z then follows (second dipolarization, marked as D2), when the B_Z value becomes larger compared to the value before the onset. More prominent B_Z enhancement is detected for C4 which preceeds C1.

To check whether the first dipolarization, D1, which is evolving Earthward, is indeed due to flux transport from the tail caused by the high speed convective bulk flow, we have compared the flux transport rate using three different methods as shown in Fig. 7: (1) 1-s average of E_Y from EFW experiment from C1 and C4 (black and blue solid lines); (2) $-V \times B$ electric field using CIS/CODIF proton moment data from C4 using V_X only (purple dotted line) and using both V_X and V_Z components (purple solid line); (3) $-V \times B$ electric field using V_X obtained from the timing of maximum B_Z from C1 and C4 (green line, where the beginning and ending of the line represent the time of the maximum B_Z from C1 and C4, respectively). Note that, due to the difference in the coordinate systems as well as the resolution of the observations, these value can be compared only as reference. Nonetheless, the maximum of the EFW and ion measurements agree within ~30% difference. The transport rate, obtained from the timing velocity is also quite consistent for the 09:07 UT and 09:21 UT event. The 09:14 event, however, started with oscillating B_Z and only the first peak (first green line in the bottom of Fig. 7b) has comparable value expected from the flux transport rate, but not the main B_Z

Fig. 8. Schematic representation of virtual spacecraft observations separated in X (fast flow direction) describing the two different types of dipolarization.

peak (second green line). It should be noted that unlike the other two events, the flux transport rate is significantly different between C1 and C4 so that simple Earthward convection was not taking place for the 09:14 event. This difference in the flux transport rate most likely suggests that flow braking is in progress between the location of C1 and C4. Signatures of transient acceleration of energetic electrons were detected associated with the temporal B_Z peaks around the 09:14 UT event (Retinò et al., 2009, manuscript in preparation) suggesting a highly disturbed current sheet at flow braking region. Based on the signatures of these three events, we can conclude that the initial dipolarization signatures are propagating Earthward and as long as the flux transport rate is not significantly changing between C1 and C4, the timing velocity of the initial B_Z enhancement of dipolarization can be well explained as simple convective transport.

5   Discussion and summary

The current sheet disturbances associated with the first dipolarization event around 09:07 UT consist of two types of oscillation. The first type is the $\sim$15 s scale oscillations, which is observed associated with the fast flow and dipolarization between 09:07 and 09:09 UT, and has a kink-mode characteristic as discussed before. The second type of the current sheet disturbance is the one observed predominantly by C2, but also by C1 and C3/C4 although the latter three spacecraft are less clear due to the larger amplitude variation from the $\sim$15 s oscillation. The opposite B_X variation below and above the equator suggests a sausage mode with a period of 2–3 min for this variation.

Theoretical models of low-frequency kink-mode oscillation of a current sheet with finite B_Z have been presented in several papers (Golovchanskaya and Maltsev, 2005; Erkaev et al., 2008; Zelenyi et al., 2009) stimulated by Cluster current sheet observations in the mid tail (e.g., Sergeev et al., 2003; Runov et al., 2005a). Compared to the previous kink mode observations by Cluster (Sergeev et al., 2003; Runov et al., 2005b; Zhang et al., 2005; Volwerk et al., 2008) in the mid-tail in a relatively thicker current sheet and during predominantly quiet intervals, the oscillation shown in this study have higher frequency, observed at a thinner current sheet but more closer to the Earth and associated with clear dipolarization and fast flows. Yet, since these kink-mode waves were reported to be elongated along X extending also toward dipolar region (Zhang et al., 2005), we may expect that these models are applicable also for our observations. Keeping in mind that the kink-mode observed in this study is associated with dipolarization, it is obvious that the effects from a finite B_Z should be taken into account considering the mechanism. Erkaev et al. (2008) proposed a model that a kink-like wave is created as a lateral displacement of the current sheet due to fast flows. This wave propagates out from the fast flow region perpendicular to the flux-tube toward flank. In this model the angular frequency ω_f can be estimated using the gradient of the field across the current sheet ($\partial B_X/\partial Z \equiv g_Z$) and along the tail axis ($\partial B_Z/\partial X \equiv g_X$) such as $\omega_f = (g_X g_Z/(4\pi\rho))^{-1/2}$, where ρ is the mass density. The mode becomes unstable when there is a negative gradient in $\partial B_Z/\partial X$ and the above expression gives then the growth time of instability, γ_f, for such case. As shown in Figs. 2 and 7, the B_Z profile associated with the dipolarization front suggests that there will appear indeed a negative gradient in B_Z along X, between C1 and C3/C4, until the flow arrives also at C3/C4, when the gradient becomes positive. Although $\partial B_Z/\partial X$ fluctuates and we have therefore not a steady situation as in the model, we can roughly estimate the expected time scale of this disturbance using the observed values. Figure 7 shows a typical value of $|\Delta B_Z/\Delta X| \sim 0.5$ nA/m^2 and $\Delta B_X/\Delta Z \sim 40$ nA/m^2 and using the observed proton number density 0.4/cc, we obtain ω_f or γ_f to be 0.14 corresponding to a period/growth time of 34 s. This is a comparable value of the estimated

flapping period before. Kink-mode oscillation was also obtained in Zelenyi et al. (2009) in a several-ion scale thin current sheet, which was the case for the observed current sheet. The theoretical prediction of the phase velocity being comparable to the drift velocity, and the wavelength to be comparable to the thickness of the current sheet is fulfilled in this observation within a factor of 6. These current sheet models therefore explain roughly temporal spatial characteristics. Yet caution is needed for more detailed comparison since the observation actually took place in a thin, but current sheet with larger B_Z than these models are generally assuming.

Both models, however, does not support the development of a sausage modes as observed before the main electrojet onset of the substorm, since both models predict predominance of the kink-mode compared to the sausage mode. Yet, considering that there are further observational evidence that thinning of the current sheet before the substorm onset can take place rather locally (or temporalily) (Asano et al., 2003), these oscillations may play an important role leading to the onset instabilities in the near-Earth current sheet.

While there are difference in the detailed response, we can summarize the three dipolarization events as illustrated in Fig. 8 for two spacecraft aligned in X (i.e. fast flow direction). The first dipolarization pulse, D1, is associated with Earthward moving dipolarization pulse transported by the Earthward fast flow but then followed by short interval with decreased level in B_Z with fluctuations. For the 09:07 UT event, this fluctuation consists of thinning and current sheet oscillation. As for the 09:14 and 09:22 UT events, the signature of decrease in B_Z contains more high frequency fluctuations. Such high-frequency fluctuations have been also reported in the dipolarization events (Shiokawa et al., 2005). In our observation the initial pulse of the dipolarization front seems to create a plasma sheet region with enhanced B_Z fluctuations. These fluctuations ceases when B_Z enhances again, i.e. the second type of dipolarization, D2. The enhancement in B_Z are more prominent and preceded by the inner spacecraft, which could be the characteristic of flux pileup. While the overall profile may therefore lead to a similar picture obtained in the MHD simulation of flux pileup (Birn and Hesse, 1996), our observation shows that the key disturbances involving FAC and therefore leading to substorms take place in the disturbed current sheet induced by the dipolarization pulse, i.e., the current sheet interval between D1 and D2.

References

Angelopoulos, V., Kennel, C. F., Coroniti, F. V., Pellat, R., Kivelson, M. G., Walker, R. J., Russell, C. T., Baumjohann, W., Feldman, W. C., and Gosling, J. T.: Statistical characteristics of bursty bulk flow events, J. Geophys. Res., 99, 21257–21280, 1994.

Asano, Y., Mukai, T., Hoshino, M., Saito, Y., Hayakawa, H., and Nagai, T.: Evolution of the thin current sheet in a substorm observed by Geotail, J. Geophys. Res., 108, 1189, doi:10.1029/2002JA009785, 2003.

Asano, Y., Shinohara, I., Retino, A., Daly, P., Kronberg, E., Takada, T., Nakamura, R., Khotyanitsev, Y., Vaivads, A., Nagai, T., Baumojohann, W., Owen, C. J., Fazakerley, A. N., Miyashita, Y., Lucek, E. A., and Rʻeme, H.: Electron acceleration signatures in the magnetotail associated with substorms, J. Geophys. Res., in preparation, 2009.

Balogh, A., Carr, C. M., Acuña, M. H., Dunlop, M. W., Beek, T. J., Brown, P., Fornacon, K.-H., Georgescu, E., Glassmeier, K.-H., Harris, J., Musmann, G., Oddy, T., and Schwingenschuh, K.: The Cluster Magnetic Field Investigation: overview of in-flight performance and initial results, Ann. Geophys., 19, 1207–1217, 2001, http://www.ann-geophys.net/19/1207/2001/.

Baumjohann, W.: Modes of convection in the magnetotail, Phys. Plasmas, 9, 9, doi:10.1063/1.1499116, 2002.

Baumjohann, W., Hesse, M., Kokubun, S., Mukai, T., Nagai, T., and Petrukovich, A. A.: Substorm dipolarization and recovery, J. Geophys. Res., 104, 24995–25000, 1999.

Birn, J. and Hesse, M.: Details of current disruption and diversion in simulations of magnetotail dynamics, J. Geophys. Res., 101, 15345–15358, 1996.

Erkaev, N. V., Semenov, V. S., and Biernat, H. K.: Magnetic double gradient mechanism for flapping oscillations of a current sheet, Geophys. Res. Lett., 35, L02111, doi:10.1029/2007GL032277, 2008.

Golovchanskaya, I. V. and Maltsev, Y. P.: On the identification of plasma sheet flapping waves observed by Cluster, Geophys. Res. Lett, 32, L02102, doi:10.1029/2004GL021552, 2005.

Gustafsson, G., André, M., Carozzi, T., Eriksson, A. I., Fälthammar, C.-G., Grard, R., Holmgren, G., Holtet, J. A., Ivchenko, N., Karlsson, T., Khotyaintsev, Y., Klimov, S., Laakso, H., Lindqvist, P.-A., Lybekk, B., Marklund, G., Mozer, F., Mursula, K., Pedersen, A., Popielawska, B., Savin, S., Stasiewicz, K., Tanskanen, P., Vaivads, A., and Wahlund, J.-E.: First results of electric field and density observations by Cluster EFW based on initial months of operation, Ann. Geophys., 19, 1219–1240, 2001, http://www.ann-geophys.net/19/1219/2001/.

Lopez, R. E., Lui, A. T. Y., Sibeck, D. G., McEntire, R. W., Zanetti, L. J., Potemra, T. A., and Krimigis, S. M.: The longitudinal and radial distribution of magnetic reconfigurations in the near-Earth magnetotail as observed by AMTE/CCE, J. Geophys. Res., 93, 997–1001, 1988.

Lui, A. T. Y., Chang, C. L., Mankofsky, A., Wong, H. K., and Winske, D.: A cross-field current instability for substorm expansions, J. Geophys. Res., 96, 11389–11401, 1991.

Nagai, T.: Observed Magnetic Substorm Signatures at Synchronous Altitude, J. Geophys. Res., 87, 4405–4417, 1982.

Nakamura, R., Baumjohann, W., Klecker, B., Bogdanova, Y., Balogh, A., Reʻme, H., Bosqued, J. M., Dandouras, I., Sauvaud, J.-A., Glassmeier, K.-H., Kistler, L., Mouikis, C., Zhang, T. L., Eichelberger, H., and Runov, A.: Motion of the dipolarization front during a flow burst event observed by Cluster, Geophys. Res. Lett., 29, 1942, doi:10.1029/2002GL015763, 2002.

Nakamura, R., Baumjohann, W., Mouikis, C., Kistler, L. M., Runov, A., Volwerk, M., Asano, Y., Vörös, Z., Zhang, T. L., Klecker, B., Rème, H., and Balogh, A.: Spatial scale of high-speed flows in the plasma sheet observed by Cluster, Geophys. Res. Lett., 31, L09894, doi:10.1029/2004GL019558, 2004.

Petrukovich, A. A., Baumjohann, W., and Nakamura, R.: Tailward and Earthward low onsets observed by Cluster in a thin current sheet, J. Geophys. Res., in review, 2009.

Rème, H., Aoustin, C., Bosqued, J. M., et al.: First multispacecraft ion measurements in and near the Earths magnetosphere with the identical Cluster ion spectrometry (CIS) experiment, Ann. Geophys., 19, 1303–1354, 2001, http://www.ann-geophys.net/19/1303/2001/.

Roux, A., Perraut, S., Robert, P., Morane, A., Pedersen, A., Korth, A., Kremser, G., Aparicio, B., Rodgers, D., and Pellinen, R.: Properties of a bifurcated current sheet observed on August 29, 2001, J. Geophys. Res., 96, 17697–17714, 1991.

Runov, A., Sergeev, V. A., Baumjohann, W., Nakamura, R., Apatenkov, S., Asano, Y., Volwerk, M., Vrs, Z., Zhang, T. L., Petrukovich, A., Balogh, A., Sauvaud, J.-A., Klecker, B., and Rème, H.: Electric current and magnetic field geometry in flapping magnetotail current sheets, Ann. Geophys., 23, 1391–1403, 2005a.

Runov, A., Sergeev, V. A., Nakamura, R., Baumjohann, W., Zhang, T. L., Asano, Y., Volwerk, M., Vörös, Z., Balogh, A., and Rème, H.: Reconstruction of the magnetotail current sheet structure using multi-point Cluster measurements, Planet. Space Sci., 53, 237–243, 2005b.

Sergeev, V., Angelopulous, V., Gosling, J. T., Cattell, C. A., and Russell, C. T.: Detection of localized, plasma-depleted flux tubes or bubbles in the midtail plasma sheet, J. Geophys. Res., 101, 10817–10826, 1996.

Sergeev, V., Runov, A., Baumjohann, W., Nakamura, R., Zhang, T. L., Volwerk, M., Balogh, A., Rème, H., Sauvaud, J.-A., and Klecker, M. A. B.: Current sheet flapping motion and structure observed by Cluster, Geophys. Res. Lett., 30, 1327, doi:10.1029/2002GL016500, 2003.

Shiokawa, K., Baumjohann, W., and Haerendel, G.: Breaking of high-speed flows in the near-Earth tail, Geophys. Res. Lett., 24, 1179–1182, 1997.

Shiokawa, K., Shinohara, I., Mukai, T., Hayakawa, H., and Cheng, C. Z.: Magnetic field fluctuations during substorm-associated dipolarizations in the nightside plasma sheet around X=−10 R_E, J. Geophys. Res., 110, A05212, doi:10.1029/2004JA010378, 2005.

Sigsbee, K., Slavin, J. A., Lepping, R. P., Szabo, A., Øieroset, M., Kaiser, M. L., Reiner, M. J., and Singer, H. J.: Statistical and superposed epoch study of dipolarization events using data from Wind perigee passes, Ann. Geophys., 23, 831–851, 2005, http://www.ann-geophys.net/23/831/2005/.

Snekvik, K., Nakamura, R., Østgaard, N., Haaland, S., and Retinò,

A.: The Hall current system revealed as a statistical significant pattern during fast flows, Ann. Geophys., 26, 3429–3437, 2008, http://www.ann-geophys.net/26/3429/2008/.

Volwerk, M., Zhang, T. L., Glassmeier, K.-H., Runov, A., Baumjohann, W., Balogh, A., Klecker, B., Rème, H., and Carr, C.: Study of waves in the magnetotail region with cluster and DSP, Adv. Space Res., 41, 1593–1597, 2008.

Zelenyi, L. M., Artemyev, A. V., Petrukovich, A. A., Nakamura, R., Malova, H. V., and Popov, V. Y.: Low frequency eigenmodes of thin anisotropic current sheets and Cluster observations, Ann. Geophys., 27, 861–868, 2009, http://www.ann-geophys.net/27/861/2009/.

Zhang, T. L., Nakamura, R., Volwerk, M., Runov, A., Baumjohann, W., Eichelberger, H. U., Carr, C., Balogh, A., Sergeev, V., Shi, J. K., and Fornacon, K.-H.: Double Star/Cluster observation of neutral sheet oscillations on 5 August 2004, Ann. Geophys., 23, 2909–2914, 2005, http://www.ann-geophys.net/23/2909/2005/.